

# A Design Method of Haptic Interface Controller Considering Transparency and Robust Stability

K.S.Eom, I.H.Suh, and B.-J.Yi

School of Electrical Eng. and Computer Science,  
Hanyang Univ., Ansan, Korea  
e-mail : kseom@incorl.hanyang.ac.kr

## Abstract

*In this paper, a transparency-optimized feedback controller with robustness is designed for multi-axis haptic device, where a disturbance observer is employed to decouple the coupling effect existing in multi-axis haptic device. A performance index for the transparency is defined in a viewpoint of admittance matching, and the optimal solution minimizing the performance index is obtained by solving  $H_2$  optimal problem. To implement a stabilizing haptic controller robust to parameteric uncertainties of haptic device, a robust stable condition using  $H_\infty$  norm derived from small gain theorem is proposed. The effectiveness of the proposed haptic control scheme has been experimentally verified for a virtual wall characterized by stiffness and damping properties.*

## 1 Introduction

Haptic interface, an important element for implementation of the virtual reality, can be considered as a device generating mechanical impedance defined by the relationship between force and velocity. The objective of haptic interface is to clearly transmit signals(force, velocity, position), and an ideal haptic system would supply a completely transparent interface between human operator and a computer generated virtual environment. Such transparency can be implemented by reducing the mass and friction effects while increasing structural rigidity and force feedback capability. However, these goals introduce conflicting requirements on actuators, structures and closed-loop implementation, and there exists difficulty in realizing the ideal transparency. On the other hand, since haptic device actively generates physical energy, instability can damage hardware and even pose a physical

threat to the human. Therefore, another important issue related to interface control is the stability of the simulation system.

Numerous attempts have been made in the recent years to maintain stable haptic interaction. Colgate et.al. proposed the passivity conditions for haptic system including virtual wall, haptic device and feedback controller[1]. From this results, the dynamic range of achievable impedance, Z-width, is defined as a measure of performance and several factors affecting Z-width have been discussed[2]. However, the result is restricted within the case employed virtual wall dynamics as the closed-loop controller. And there was not discussed design method of feedback controller. Adams and Hannaford represented the haptic interface as a linear two-port with terminals for a human operator and a virtual environment, and proposed the unconditionally stable condition that the two-port network should be passive and a design procedure using virtual coupling to guarantee the stability[3, 4]. Although this approach has the advantage that the design problem can be decoupled from the design of virtual environment, the solution is not the best in the viewpoint of transparency. Moreover, because the passivity condition depends on the dynamics of haptic display, the design problem may not be applied to the case of multi-axis haptic system whose dynamics are changing according to the configuration of haptic system.

In this paper, a controller design method is proposed for multi-axis haptic interface considering transparency and robust stability. Specifically, a disturbance observer is applied to each axis in Cartesian space to obtain a simple equivalent robot dynamics(SERD) being represented as independent mass-damper system. In order to design a transparent-optimized feedback controller, a performance index representing the transparency as performance mea-

sure is defined in a viewpoint of admittance matching, and the optimal solution which is minimizing the performance index is obtained by solving  $H_2$  optimal problem. To implement the robust stabilizing haptic controller to the parameteric uncertainties of haptic device, a robust stable condition using  $H_\infty$  norm from small gain theorem is derived. To verify the performance of the proposed haptic controller design scheme, experimental results are illustrated for virtual wall consisting of stiffness and damping factor.

## 2 Disturbance Observer-Based Haptic System Modeling

Haptic display can be considered as multi-axis robot manipulator. Consider dynamics of an  $n$  link robot manipulator given by a set of highly nonlinear and coupled differential equations as

$$\tau = M(q)\ddot{q} + V(q, \dot{q}) + G(q) + B\dot{q} + H(\dot{q}), \quad (1)$$

where  $M(q)$  and  $B$  are the  $n \times n$  inertia matrix and viscous friction constant matrix, respectively. And  $V(q, \dot{q})$ ,  $G(q)$ , and  $H(\dot{q})$  are, respectively, the  $n \times 1$  vectors of the Coriolis and centrifugal forces, the gravity loading and Coulomb friction force.  $\tau = [\tau_1 \cdots \tau_n]^T$  is the  $n \times 1$  torque vector applied to the joint of robot manipulator.  $q$ ,  $\dot{q}$ ,  $\ddot{q}$  are the  $n \times 1$  vectors representing angular position, velocity and acceleration, respectively. The representation of the dynamics in Cartesian space using Jacobian matrix can be written as

$$F = M_x(q)\ddot{x} + V_x(q, \dot{q}) + G_x(q) + B_x\dot{x} + H_x(\dot{q}), \quad (2)$$

$$M_x(q) = J^{-T}(q)M(q)J^{-1}(q),$$

$$V_x(q) = J^{-T}(q)(V(q, \dot{q}) - M(q)J^{-1}(q)\dot{J}(q)\dot{q}),$$

$$G_x(q) = J^{-T}(q)G(q),$$

$$B_x(q, \dot{q}) = J^{-T}(q)BJ^{-1}(q),$$

$$H_x(q, \dot{q}) = J^{-T}(q)H(\dot{q}),$$

where  $J(q)$  is Jacobian matrix and  $\dot{J}(q)$  is the derivative of  $J(q)$ . And,  $x$ ,  $\dot{x}$ ,  $\ddot{x}$  are the  $m \times 1$  vectors representing position, velocity and acceleration in Cartesian space, respectively. Now the robot dynamics in Eq.(2) can be written as a fixed mass term and viscous friction term plus an equivalent disturbance force given by

$$F = \bar{M}_x\ddot{x} + \bar{B}_x\dot{x} + F_{xd}(q, \dot{q}), \quad (3)$$

where  $\bar{M}_x \triangleq \text{diag}\{\bar{M}_{11} \cdots \bar{M}_{mm}\}$  is the  $m \times m$  diagonal matrix. Here,  $\bar{M}_{ii}$  is the constant valued nominal mass term of the  $i$ th axis which can be approximately measured by frequency response. Specifically,

a frequency response for the  $i$ th axis can be obtained by locking all other axis except the  $i$ th axis. Then, by assuming that the dynamics of the  $i$ th axis can be treated as  $F_i = \bar{M}_{ii}\ddot{x}_i + \bar{B}_{ii}\dot{x}_i$ ,  $\bar{M}_{ii}$  and  $\bar{B}_{ii}$  can be experimentally measured by using a frequency response for the force input and the velocity output. In Eq.(3),  $F_{xd}(q, \dot{q}) \triangleq [F_{1xd}, \cdots, F_{mxd}]^T$  is the  $m \times 1$  vector implying equivalent disturbance including all the unmodeled dynamics, such as nonlinearity, coupling effect and payload uncertainty.  $F_{xd}$  can be rewritten as

$$F_{xd} = (M_x(q) - \bar{M}_x)\ddot{x} + V_x(q, \dot{q}) + G_x(q) + H_x(\dot{q}). \quad (4)$$

If the equivalent disturbance in Eq.(4) can be obtained, dynamics of each axis can be decoupled by eliminating the equivalent disturbance. The equivalent disturbance can be estimated by disturbance observer [5, 6] and can be suppressed by adding the estimated disturbance signal to the control input. Fig.1 shows a structure of the disturbance observer for the  $i$ th single axis which is based on inverse model of nominal plant. In Fig.1,  $P_{in}$  is the nominal plant of the real system  $P_i(s)$  where  $P_{in}$  is given as  $1/(\bar{M}_{ii}s + \bar{B}_{ii})$ , and  $Q_i(s)$  is a low pass filter which is employed to realize  $P_{in}^{-1}(s)$  and to reduce the effect of measurement noise. From the relationship between input and output in Fig.1, if the magnitude of  $Q_i(s)$  is approximately equal to one, the real plant acts as the nominal plant, otherwise as real plant. This implies that for a disturbance signal whose maximum frequency is lower than cut-off frequency of  $Q_i(s)$ , the disturbance signal is effectively rejected and the real plant behaves as a nominal plant. Therefore, if such a disturbance observer is employed for every axis, then the robot dynamics in Cartesian space can be considered as the simple equivalent dynamic(SERD) system given by

$$F = \bar{M}_x\ddot{x} + \bar{B}_x\dot{x}. \quad (5)$$

From Eq.(5), the multi-DOF haptic model employing disturbance observer can be simplified to several one DOF haptic device model sketched in Fig.2 Now, without loss of generality, consider a single DOF rigid manipulator as haptic device whose dynamics is given by

$$m\dot{v}_d + bv_d = F_h - F_d, v_d = v_h. \quad (6)$$

Here  $v_h$  and  $v_d$  are, respectively, the velocity of the human operator at the point of contact with the device and the velocity of the device at the point of actuation.  $F_h$  is the force applied by human operator at the point of contact and  $F_d$  is the force applied by the device at

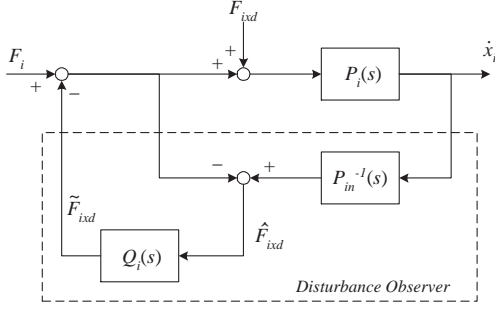


Figure 1: A structure of disturbance observer.

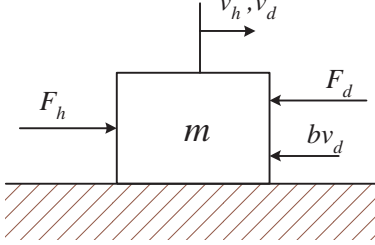


Figure 2: One DOF haptic device model

the point of acutation. For impedance model of haptic interaction where the force are applied to the human operator in response to measured displacement, the continuous time transfer function from  $F_h$  to  $v_h$  can be found by taking the Laplace transform of Eq.(6) as follows;

$$P(s) = \frac{1}{ms + b}. \quad (7)$$

The command to implement a virtual environment should be sent to actuator through digital-to-analog converter which is modeled by putting the transfer function in Eq.(7) in series with a zero-order holder. The effect of zero-order holder is approximated by a low pass filter with unity steady-state gain and 90 degrees phase lag at the Nyquist frequency. The spring-damper model is typically employed as a virtual wall and the transfer function from the velocity at the contact point to the command force is given by

$$V(s) = \frac{K + Bs}{s}. \quad (8)$$

In Eq.(8),  $K$  and  $B$  are the spring constant and damping coefficient of virtual wall, respectively. The block diagram of haptic interface is depicted in Fig.3. The feedback controller,  $C(s)$ , is generally implemented by using virtual wall dynamics to be represented. The performance of haptic interface can be described in terms of transparency which can be defined as the

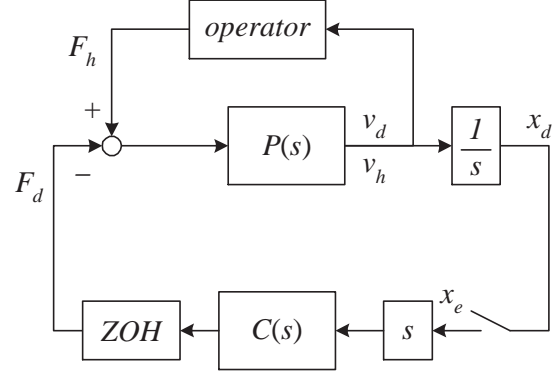


Figure 3: Block diagram of haptic interface

quality of impedance or admittance matching. The impedance and admittance are the relationships between velocities and forces. Haptic interface has perfect transparency when the admittance/impedance of virtual wall is equal to that of force feedback device[7]. From Fig.3, the transmitted admittance of the closed loop haptic system can be derived as Eq.(9).

$$Y_t(s) = \frac{P(s)}{1 + ZOH(s)P(s)C(s)}. \quad (9)$$

Colgate and Brown[2] proposed using the Z-width performance measure for haptic system. The Z-width is defined as the achievable range of impedances which the haptic interface can stably present to the operator. However, when the virtual environment to be implemented is out of the range of Z-width, stability as well as transparency cannot be guaranteed. For this case, an admittance plot in frequency domain is depicted in Fig.4. The admittance plot for virtual wall has high pass filter dynamics and the unstable haptic system has the same response in low frequency region. However, the overall system has chattering or unstable characteristic due to the peak resonance. In this case, the best solution is to design the haptic feedback controller,  $C(s)$ , such that the peak resonance is excluded. In the next section, a design method of stabilized and transparency-optimized feedback controller will be described.

### 3 Transparency-Optimized Haptic Interface

In the design of haptic feedback controller, the objective is to find  $C(s)$  while not only stabilizing the haptic feedback system but also minimizing the admittance error between virtual wall to be represented

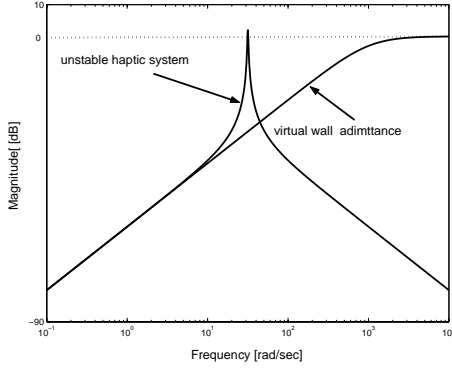


Figure 4: Typical admittance plot

and haptic feedback system. The performance measure for the transparency can be defined as integral terms of the squared output error for the same input force between the virtual wall and haptic feedback system. Eq.(10) shows a performance index in time domain output and it can be transformed to frequency domain performance measure by Parseval's theorem as shown in Eq.(11).

$$J = \int_0^{\infty} (v_v(t) - v_h(t))^2 dt. \quad (10)$$

$$\begin{aligned} J &= \|w_1(Y_v - Y_t)\|_2^2 \\ &= \frac{1}{2\pi} \int_{-\infty}^{\infty} |w_1(jw)(Y_v(jw) - Y_t(jw))|^2 dw, \end{aligned} \quad (11)$$

where  $Y_v(s)$  is the admittance function of virtual wall and it can be represented as Eq.(8).  $w_1(s)$  is weighting function which can be properly determined according to input signal [8]. For the performance measure representing transparency,  $w_1(s)$  may be chosen a low pass filter because the input force signal exerted by human operator,  $F_h$ , is a frequency limited signal.

The design problem of the optimal controller minimizing performance measure in Eq.(11) is to find  $H_2$  optimal solution. If the feedback controller has the same form as the dynamics of the virtual wall,  $C(s)$  can be written as

$$C(s) = B_c + \frac{K_c}{s}, \quad (12)$$

where  $K_c$  and  $B_c$  are the feedback gains for position and velocity, respectively. When the position feedback gain,  $K_c$ , is equal to the stiffness coefficient of virtual wall,  $K$ , the steady state error between the position of haptic feed system and virtual wall goes to zero. Thus,  $K_c$  value should be set  $K$ . It is implied that if  $K_c$  is

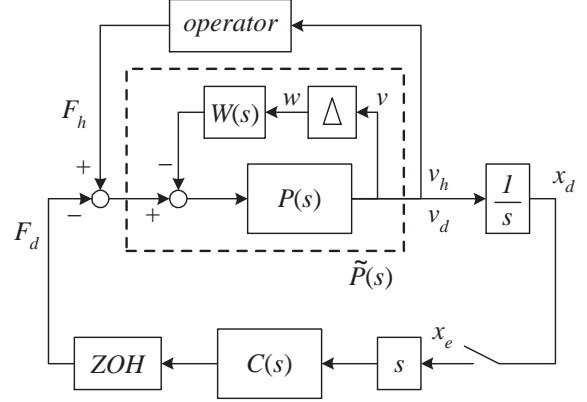


Figure 5: Block diagram of perturbed haptic system

not equal to  $K$ , the performance measure defined in Eq.(11) is not bounded and the  $H_2$  optimal solution is meaningless. As a result, the  $H_2$  optimal controller design problem can be reduced to a simple parameter optimization problem to find  $B_c$  minimizing the performance index.

If the nominal model of the haptic device defined in Eq.(7) has parametric uncertainties, the nominal performance cannot be guaranteed. Suppose that the nominal plant parameters in Eq.(7) are  $m$  and  $b$ , and consider perturbed haptic device transfer function of the form

$$\tilde{P}(s) = \frac{1}{m(1 + \alpha\Delta)s + b(1 + \beta\Delta)}. \quad (13)$$

Here  $\alpha$  and  $\beta$  are a constant values and  $\Delta$  is a variable satisfying  $-1 \leq \Delta \leq 1$ . Eq.(13) can be rewritten for nominal plant  $P(s)$  and a fixed transfer function  $W(s)$  as shown in Eq.(14), and the block diagram of the haptic feedback system with uncertainties is shown in Fig.5, where

$$\tilde{P}(s) = \frac{P(s)}{1 + W(s)\Delta P(s)}, \quad (14)$$

and

$$W(s) = \alpha ms + \beta b. \quad (15)$$

For deriving the robust stability condition using the small-gain theorem, the relationship between the input  $w$  and the output  $v$  can be easily obtained by

$$L(s) \triangleq \frac{v}{w} = \frac{-W(s)P(s)}{1 + ZOH(s)P(s)C(s)}. \quad (16)$$

And the robust stability condition can be summarized as follows[9].

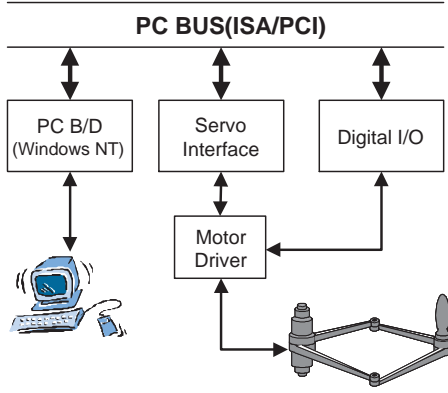


Figure 6: Experimental Setup

*Theorem 1 - The stable haptic feedback controller  $C(s)$  for the nominal plant is robust stable for the parametric uncertainties if and only if the following condition holds;*

$$\|L(s)\|_{\infty} \leq 1. \quad (17)$$

The optimal feedback controller design problem is to find  $B_c$  minimizing the performance index under the constraint in Eq.(17). However, it is difficult to analytically solve this problem. Another choice to obtain the same result is a numerical recursive method that at first, the solution minimizing the performance index for nominal haptic system is determined and the robust stable condition for the solution is checked.

## 4 Experimental Results

All experiments are performed by employing a 2 DOF parallel type haptic device whose link length is  $0.2[m]$ . The device powered by two AC servo motor with PWM amplifier and the each motor shaft is equipped with a encoder for position sensing. The voltage input to the amplifier for current command are provided by a 12-bit D/A converter. The control algorithm is implemented using C language and tested our prototype controller, where a industrial PC board embedded Windows NT are used as sketched in Fig.6 and the sampling rate is set to  $1[msec]$  for digital control.

The nominal values of mass and viscous friction coefficient of the haptic in the direction to the virtual wall are, respectively, obtained by the frequency response in Cartesian space as  $m = 0.01[Kg]$  and  $b = 0.022[Nsec/m]$ . The stiffness and damping factors of the virtual wall to be simulated are given by

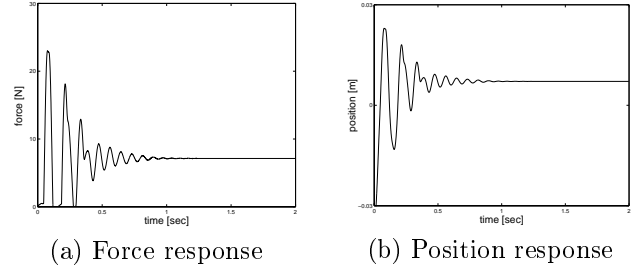


Figure 7: Force and position response for the case of general feedback controller

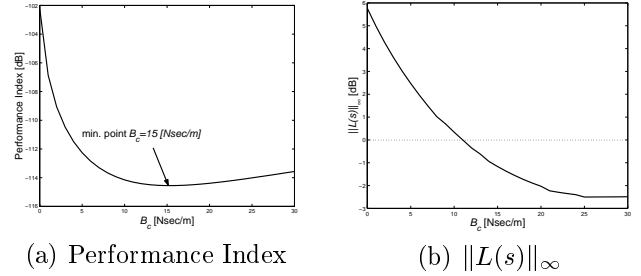


Figure 8: Performance index and  $\|L(s)\|_{\infty}$  vs  $B_c$

$K = 1000[N/m]$  and  $B = 1[Nsec/m]$ , respectively. The force command of the human operator is exerted as  $-5[N]$ . When the virtual wall dynamics as the feedback controller is employed, the force response and the position response are plotted in Fig.7. It is observed from Fig.7 that there exists oscillation in transient response due to admittance mismatch.

In order to determine the optimal gain  $B_c$  in the viewpoint of transparency for given virtual wall, the weighted performance measure defined in Eq.(11) for variations of  $B_c$  is plotted in Fig.8. From this figure, when  $B_c$  is set to  $15[Nsec/m]$ , the admittance error is minimized and the operator can feel the similar admit-

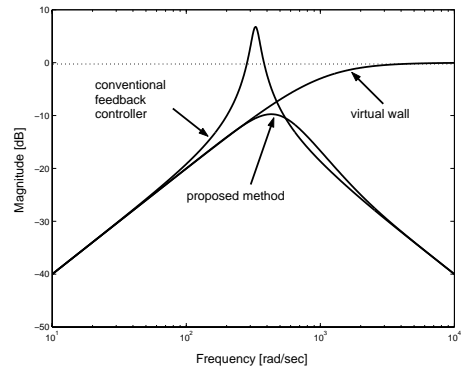


Figure 9: Admittance Response

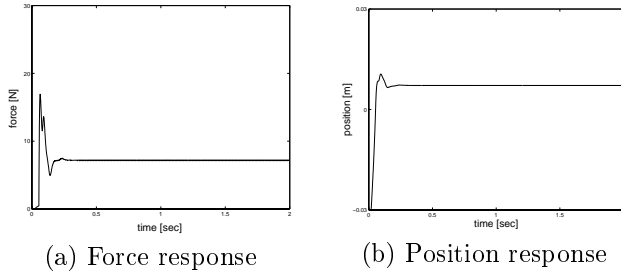


Figure 10: Force and position response for the case of proposed feedback controller

tance under the given environment (haptic device). To guarantee robust stability for parametric uncertainties when the uncertain degrees in Eq.(15) are given by  $\alpha = 0.5$  and  $\beta = 0.5$ ,  $\|L(s)\|_\infty$  plot is shown in Fig.8.  $\alpha = 0.5$  and  $\beta = 0.5$  imply that the perturbed mass and damping factor are bounded by  $0.005 \leq \tilde{m} \leq 0.015 [Kg]$  and  $0.011 \leq \tilde{b} \leq 0.033 [Nsec/m]$ . Note that  $H_\infty$  gain smaller than unity guarantees the robust stability. But,  $B_c$  of  $1 [Nsec/m]$  results in 4.5dB  $H_\infty$  gain, and thus robust stability cannot be maintained. On the other hand,  $B_c$  minimizing the performance index satisfies the robust stability condition. The admittance in frequency domain is shown in Fig.9, and it can be observed that the peak resonance affecting the chattering or unstable characteristic has disappeared. The force and position responses for the admittance matching solution is depicted in Fig.10.

## 5 Concluding Remarks

A controller design methodology was suggested for multi-axis haptic display considering transparency and robust stability. To exclude the coupling effect existing in multi-axis haptic display, the equivalent disturbance in Cartesian space including modeling uncertainties and coupling effect was derived and can be effectively removed using disturbance observer. Thus, haptic model employing disturbance observer could be simplified to several one DOF haptic device model. A performance index for the transparency-optimized haptic interface was defined in a viewpoint of admittance matching, and the optimal solution minimizing the performance index was obtained by solving  $H_2$  optimal problem. And robust stabilizing condition using  $H_\infty$  norm is described. As one of our future works, 6-DOF haptic system with parallel structure in under investigation.

## References

- [1] J. E. Colgate and G. Schenkel, "Passivity of a Class of Sampled-Data System : Application to Haptic Interface," *Proceedings of American Control Conference*, Baltimore, pp.3236-3240, 1994
- [2] J. E. Colgate and J. M. Brown, "Factors Affecting the Z-width of a Haptic Display," *Proceedings of IEEE Int. Conf. on Robotics and Automation*, Los Alamitos, CA, pp.3205-3210, 1994
- [3] R. J. Adams and B. Hannaford, "A two-port Framework for the Design of Unconditionally Stable Haptic Interface," *Proceedings of 1998 IEEE/RSJ Int. Conf. on Intelligent Robotics and System*, pp.1254-1259, 1998
- [4] R. J. Adams and B. Hannaford, "Stable Haptic Interaction with Virtual Environment," *IEEE Trans. on Robotics and Automation*, vol. 15, no. 3, pp. 465-474, 1999.
- [5] T. Umeno and Y. Hori, "Robust speed control of dc servomotors using modern two degrees-of-freedom controller design," *IEEE Trans. on Industrial Electronics*, vol. 38, no. 5, pp. 363-368, 1991.
- [6] H. S. Lee, "Robust Digital Tracking Controllers for High-Speed/High-Accuracy Positioning System," *Ph.D. Dissertation*, U.C Berkeley, 1994
- [7] D. A. Lawrence, "Stability and Transparency in Bilateral Teleoperation," *IEEE Trans. on Robotics and Automation*, vol.9, no.5, pp.622-637, 1993
- [8] M. Morari and E. Zafiriou, *Robust Process Control*, Prentics Hall, 1989
- [9] J. C. Doyle, B. A. Francis and A. R. Tannenbaum, *Feedback Control Theory*, Macmillan Publishing Company, 1992
- [10] K. S. Eom, I. H. Suh, W. K. Chung and S.-R. Oh, "Disturbance Observer Based Force Control of Robot Manipulator without Force Sensor," *Proc. of IEEE Intl. Conf. on Robotics and Automation*, Leuven, Belgium, pp.3012-3017, 1998
- [11] K. S. Eom, I. H. Suh and W. K. Chung, "Disturbance Observer based Path Tracking Control of Robot Manipulator considering Torque Saturation," *Proc. of Intl. Conf. on Advanced Robotics*, Monterey, pp.651-657, 1997